Supplemental Materials

Molecular Biology of the Cell

Majumdar et al.

Supplemental Figure 1: SDS-PAGE of proteins used in this study
Purity of different constructs and mutants as analyzed by SDS-PAGE. Molecular weight markers are in kDa. Tubulin concentration is 3 μM; all others are 10 μM.

Supplemental Figure 2: Affinity of TOG2 to unpolymerized tubulin determined by MST

Binding of TOG2 to unpolymerized tubulin analyzed by microscale thermophoresis. [Tubulin] in all samples was 40 nM and TOG added in a 15-point 1:1 dilution series with highest concentration at 120 μM. Normalized fluorescence scans for different TOG concentrations show changes in fluorescent counts over time showing pre-IR, IR-on and post-IR phases (top panel). Aberrant thermophoresis was detected for high [TOG2] samples and excluded from the binding isotherm (not shown). The data showing relative change in fluorescence versus protein concentration fit well to a single-site binding model (bottom panel), yielding K_D = 2.6 μM.

Supplemental Figure 3: Comparing Stu1-TOG2 to 'arched' and 'flat' TOG domains
Different configurations of the tubulin-binding interface on selected TOG domains. In each panel a cartoon representation of a given TOG is shown inside of its solvent-accessible surface (transparent grey). Evolutionarily conserved W,R residues implicated in tubulin binding are shown in space-filling representation at the 'top' and 'bottom' of the tubulin binding surface. Line drawings emphasize the shape of the tubulin-binding surface and the important W,R residues. Stu1-TOG2 does not show the 'arched' configuration observed for hCLASP1. The arrow on the Stu1-TOG2 panel indicates the 'retraction' of the conserved Tryptophan.
Top left: CLASP-family TOG: hCLASP1, PDB code 4K92, grey.

Top right: polymerase-family TOG: Stu2-TOG2, PDB code 4U3J, blue.
Bottom: CLASP-family TOG: Stu1-TOG2, PDB code 6COK, this study, orange.

Supplemental Figure 4: TOG1 does not affect MT dynamics
Quantification of the microtubule dynamics in presence of 200 nM TOG1 (in black; data for Control, grey, and TOG2, red, are reproduced from Figure 5). From left to right: growing rates do not change substantially (control: 17.9 ± 0.2 μm/hr, n = 245; +TOG1: 16.8 ± 0.3 μm/hr, n = 38; for comparison +TOG2: 18.8 ± 0.3 μm/hr, n = 126); in contrast to the anti-catastrophe activity we observed for Stu1-TOG2, no change in catastrophe frequency is observed in the presence of TOG1 (control: 0.098 {0.094, 0.100} min^{-1}, n = 57, 160; +TOG2: 0.025 {0.024, 0.027} min^{-1}, n = 44, 38; +TOG1: 0.092 min^{-1}, n = 36). No rescues were observed in the presence of TOG1 (control: no rescues; +TOG1: no rescues; for comparison +TOG2: 19 {18, 20} min^{-1}, n = 21, 16 rescues). Values reported for control and +TOG2 are weighted average over two independent experiments with the averages from each separate experiment given in braces to provide a measure of experimental variation, followed by number of observed events in

each trial. Values for +TOG1 are from a single trial.

Supplemental Figure 5: Folding and stability of Stu1-TOG2 mutants assessed by CD
A. CD spectra of TOG2 and mutants showing characteristic secondary structural features in the far-UV. Amplitudes of the spectra vary due to differences in concentrations
B. Normalized spectra show nearly perfect overlap indicating that the point mutations do not cause large-scale structural changes
C. Melting curves (CD monitored at 221nm) in response to heating from 298.15 K to 368.15 K. Mutants show similar melting transition to wildtype TOG2, with the R386A mutant being slightly destabilized (see **D** for melting temperatures derived from these curves)
D. Apparent T_m for wildtype and mutant TOG2. Point mutations do not have significant effect on protein stability

Supplemental Figure 6: Affinity of Stu1-TOG2 W339,R525A to MT lattice
A. Stu1-TOG2 W339A,R525A binds very weakly to MT lattice. Binding isotherm of Stu1-TOG2 W339A,R525A (purple) and TOG2 (red) to MT lattice showing normalized intensity on the lattice versus concentration and fit to a single-site binding model. TOG2 data reproduced from Figure 2. Concentrations of Stu1-TOG2 W339A,R525A were 0.5, 1, 2, 5, 10, 15, 20 μM. n = 15 scans per concentration for a single Stu1-TOG2 W339A,R525A titration (purple).

Top right: polymerase-family TOG: Stu2-TOG2, PDB code 4U3J, blue.
Bottom: CLASP-family TOG: Stu1-TOG2, PDB code 6COK, this study, orange.
Supplemental Figure 4: TOG1 does not affect MT dynamics
Quantification of the microtubule dynamics in presence of 200 nM TOG1 (in black; data for Control, grey, and TOG2, red, are reproduced from Figure 5). From left to right: growing rates do not change substantially (control: 17.9 ± 0.2 μm/hr, n = 245; +TOG1: 16.8 ± 0.3 μm/hr, n = 38; for comparison +TOG2: 18.8 ± 0.3 μm/hr, n = 126); in contrast to the anti-catastrophe activity we observed for Stu1-TOG2, no change in catastrophe frequency is observed in the presence of TOG1 (control: 0.098 {0.094, 0.100} min^{-1}, n = 57, 160; +TOG2: 0.025 {0.024, 0.027} min^{-1}, n = 44, 38; +TOG1: 0.092 min^{-1}, n = 36). No rescues were observed in the presence of TOG1 (control: no rescues; +TOG1: no rescues; for comparison +TOG2: 19 {18, 20} min^{-1}, n = 21, 16 rescues). Values reported for control and +TOG2 are weighted average over two independent experiments with the averages from each separate experiment given in braces to provide a measure of experimental variation, followed by number of observed events in each trial. Values for +TOG1 are from a single trial.

Supplemental Figure 5: Folding and stability of Stu1-TOG2 mutants assessed by CD
A. CD spectra of TOG2 and mutants showing characteristic secondary structural features in the far-UV. Amplitudes of the spectra vary due to differences in concentrations

B. Normalized spectra show nearly perfect overlap indicating that the point mutations do not cause large-scale structural changes
C. Melting curves (CD monitored at 221nm) in response to heating from 298.15 K to 368.15 K. Mutants show similar melting transition to wildtype TOG2, with the R386A mutant being slightly destabilized (see **D** for melting temperatures derived from these curves)
D. Apparent T_m for wildtype and mutant TOG2. Point mutations do not have significant effect on protein stability

Supplemental Figure 6: Affinity of Stu1-TOG2 W339,R525A to MT lattice
A. Stu1-TOG2 W339A,R525A binds very weakly to MT lattice. Binding isotherm of Stu1-TOG2 W339A,R525A (purple) and TOG2 (red) to MT lattice showing normalized intensity on the lattice versus concentration and fit to a single-site binding model. TOG2 data reproduced from Figure 2. Concentrations of Stu1-TOG2 W339A,R525A were 0.5, 1, 2, 5, 10, 15, 20 μM. n = 15 scans per concentration for a single Stu1-TOG2 W339A,R525A titration (purple).

Sup. Figure 1

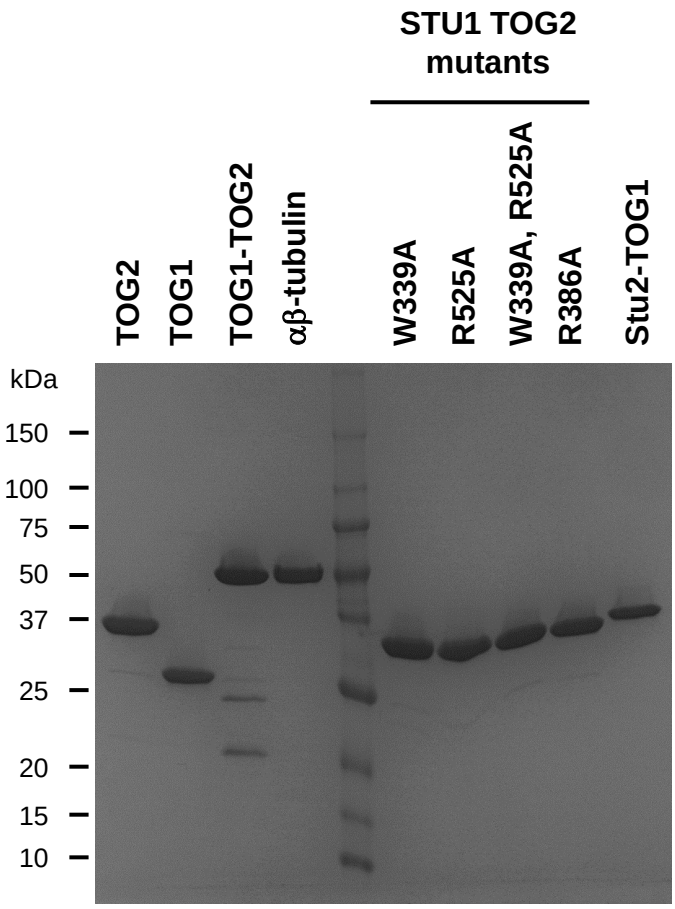
STU1 TOG2 mutants
TOG2
TOG1
TOG1-TOG2
αβ-tubulin
W339A
R525A
W339A, R525A
R386A
Stu2-TOG1
kDa
150
100
75
50
37
25
20
15
10

Sup. Figure 2

K_D = 2.6 [1.6, 4.6] µM

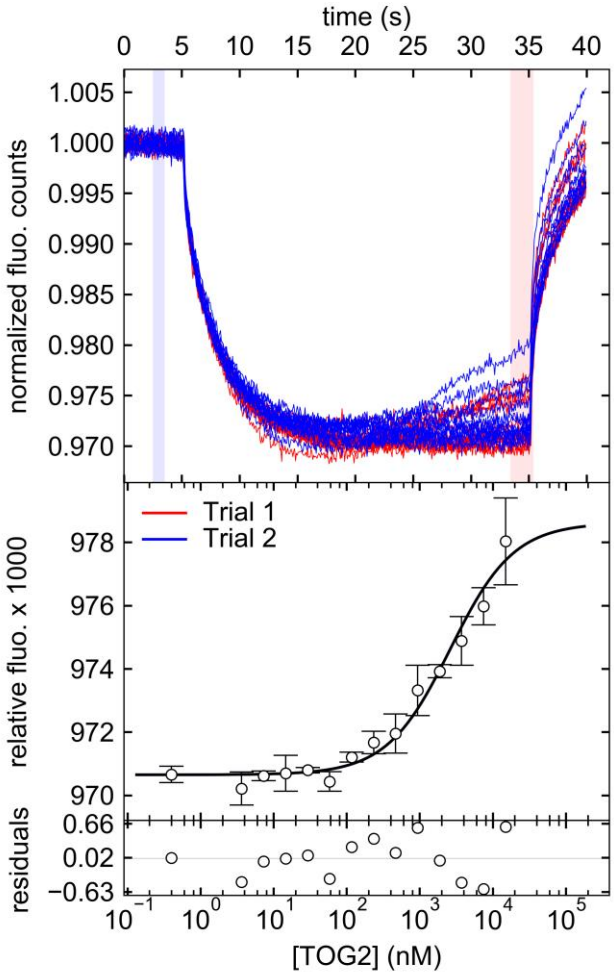

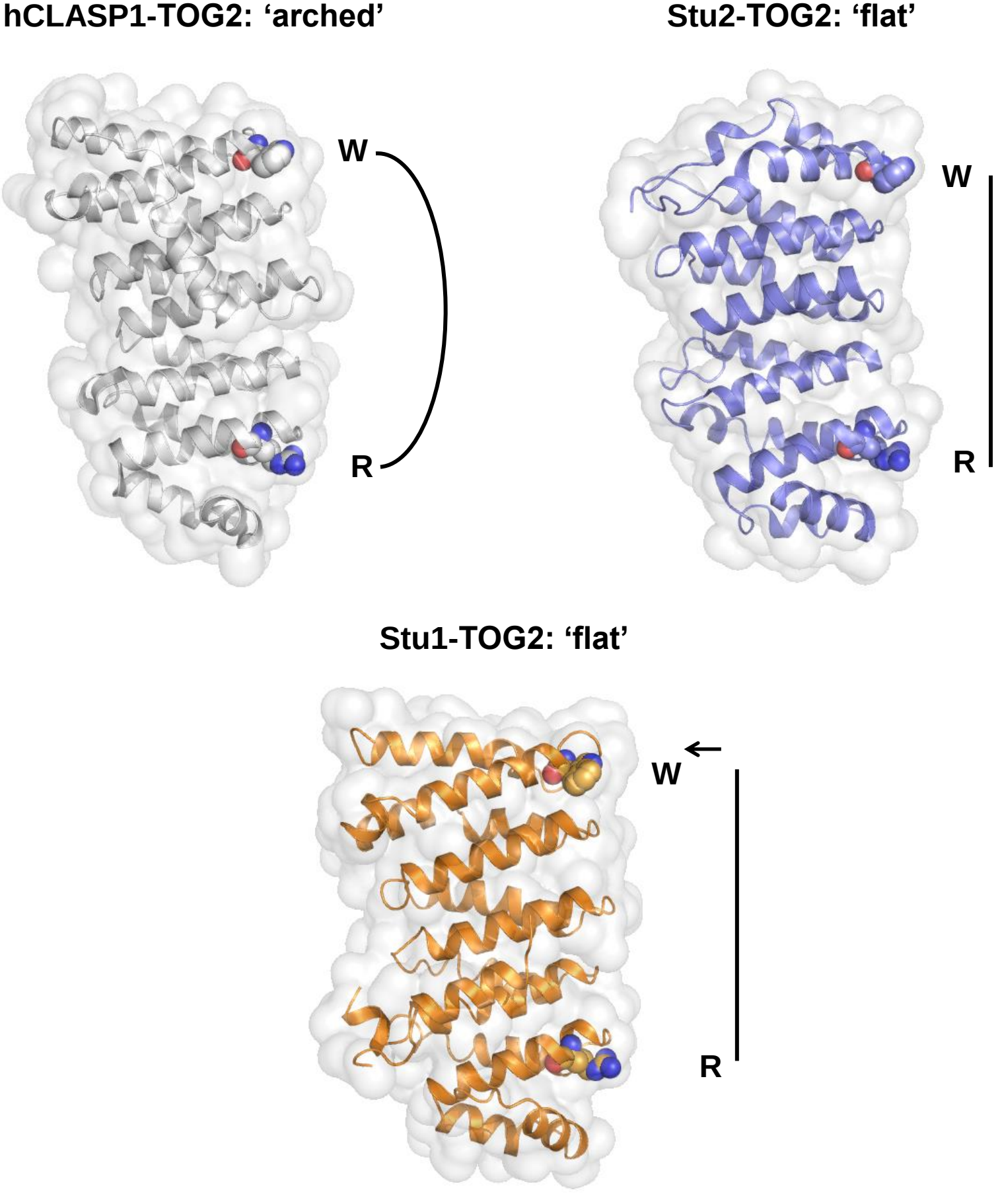
hCLASP1-TOG2: ‘arched’
W
R
Stu2-TOG2: ‘flat’
W
R
Stu1-TOG2: ‘flat’
W
R

Sup. Figure 4

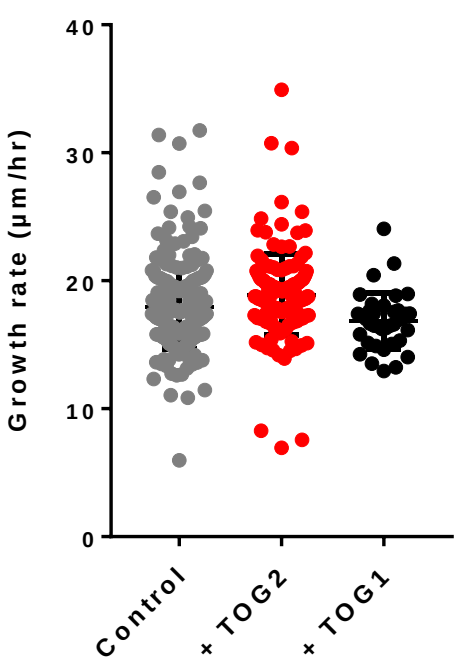
Growth rate (µm/hr)
40
30
20
10
0
Control
+ TOG2
+ TOG1

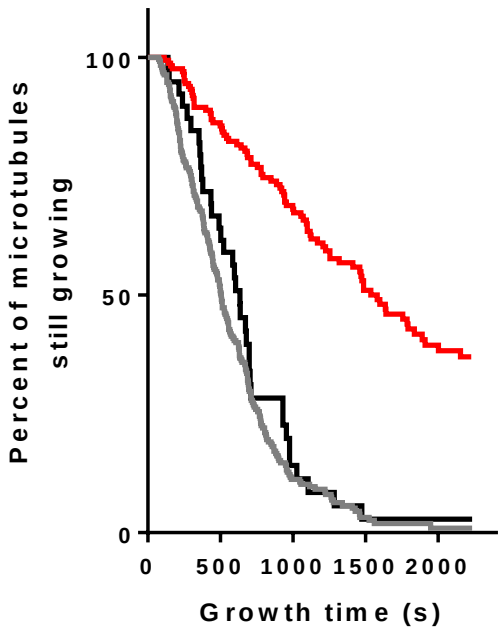
Percent of microtubules still growing
100
50
0
0
500
1000
1500
2000
Growth time (s)

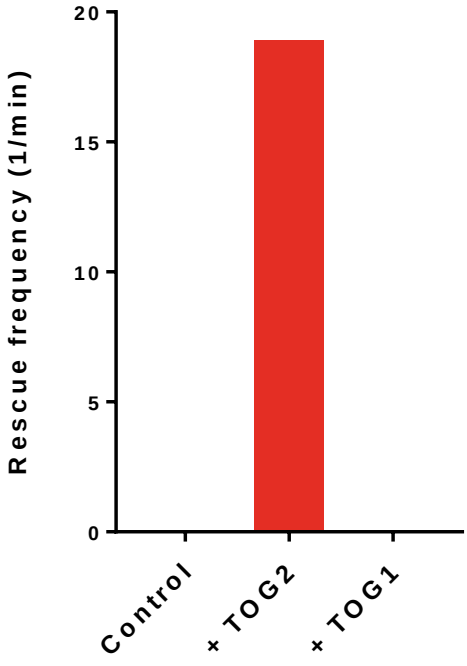
Rescue frequency (1/min)
20
15
10
5
0
Control
+ TOG2
+ TOG1

Sup. Figure 5

A

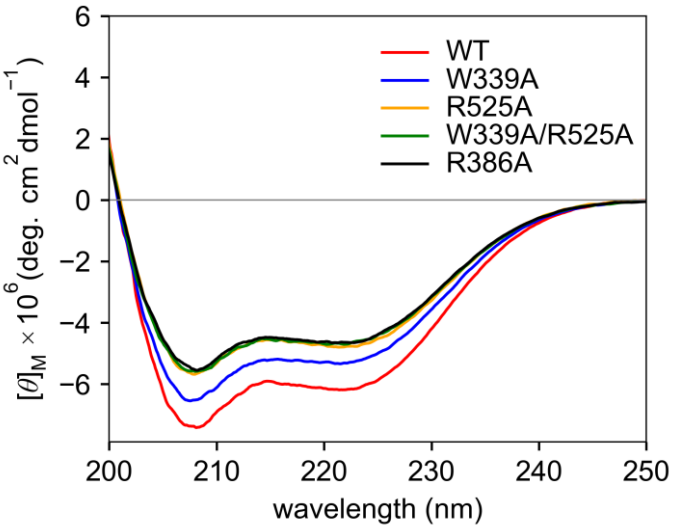

B

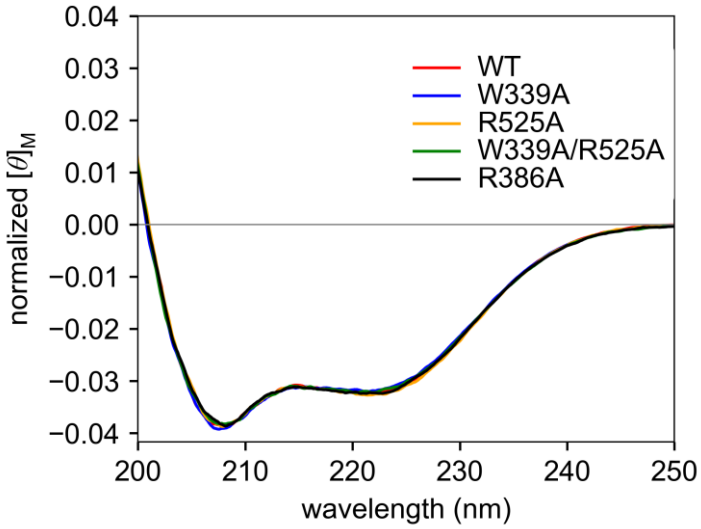

C

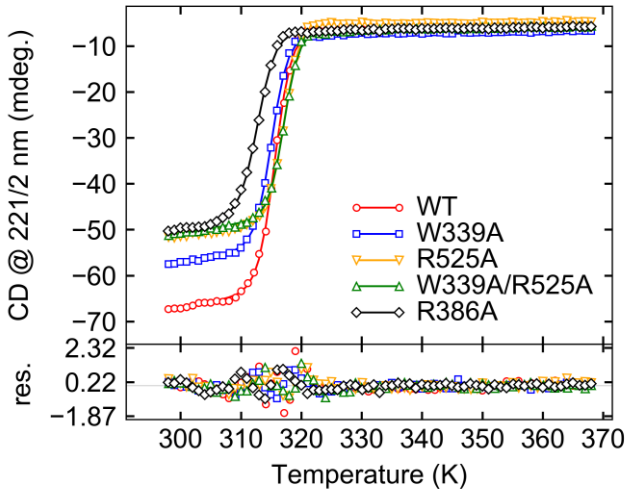

D

STU1-TOG2 construct	Apparent T_m (K)
Wild-type	317.5
W339A	315.1
R525A	317.2
W339A/R525A	317.2
R386A	312.8

Sup. Figure 6

A

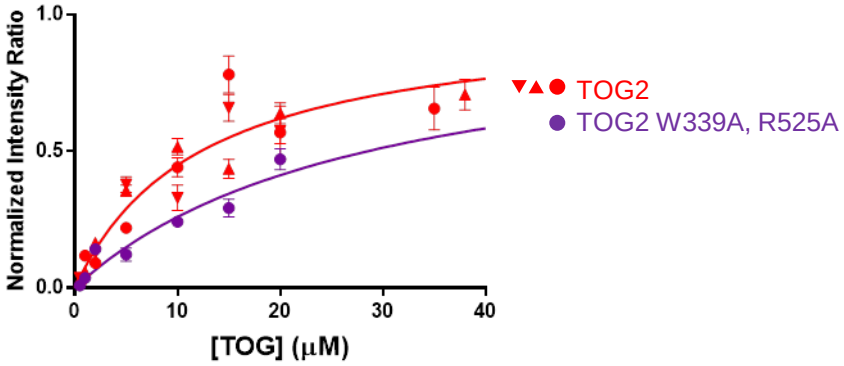

B

	K_D (µM)
TOG2	12 ± 3
TOG2 W339A, R525A	29 ± 8

Sup. Figure 7

A

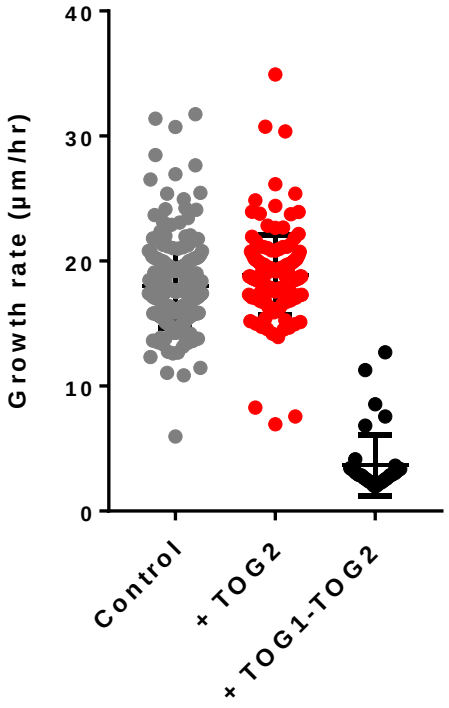

B

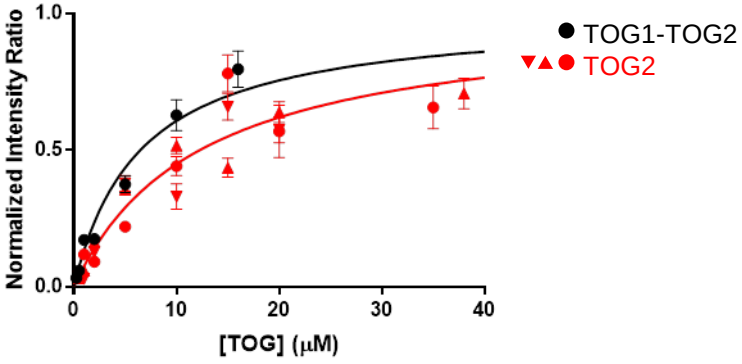

	K_D (µM)
TOG2	12 ± 3
TOG1-TOG2	7 ± 2

C

AUC: K_D = 720 [670, 780] nM

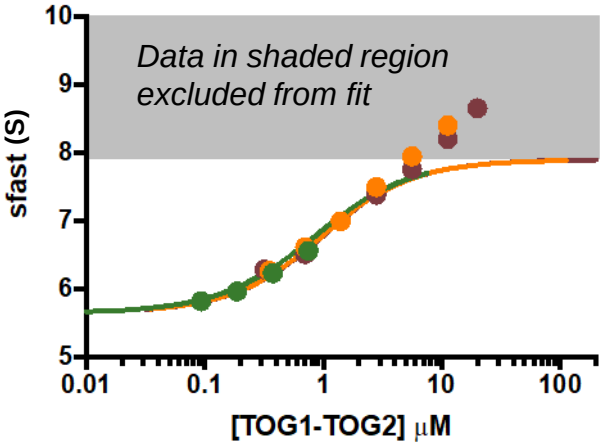

MST: K_D = 130 [100, 170] nM